Self-Focusing of Laser Light and Stimulated Scattering Processes in Transparent and Absorbing Liquids:

1. Self-Focusing

M. MAIER, O. RAHN, and G. WENDL *

Physik-Department der Technischen Universität München

(Z. Naturforsch. **25 a**, 1868—1879 [1970]; received 26 September 1970)

The spatial and temporal development of self-focusing of light pulses is investigated. The beam diameter in CS_2 and molten para-di-chlorobenzene decreases with increasing incident laser power to small values in good agreement with theory. The strong influence of beam divergence, nonlinearity of refractive index, and absorption on self-focusing action is found to agree well with numerical calculations. It is shown that both backward stimulated Brillouin and Raman scattering terminate the self-focusing process.

I. Introduction

If light of high intensity propagates through a medium with an intensity-dependent refractive index, self-focusing occurs [1–3]. The diameter of the light beam shrinks to a small limiting value. Depending on the experimental conditions either a moving focus [4] is observed, or the light is found to propagate in filaments of small diameter [5]. Most of the experimental investigations are concerned with these intense self-trapped light filaments [6]. Only recently experimental results on the self-focusing process have been reported. MCALLISTER et al. [7] found pulse shaping during the self-focusing process of the laser beam; LOY and SHEN [4] showed that, with increasing laser power, the focused beam diameter shrank from 50 μ to the limiting size (5 μ in CS_2).

High light intensities produced by self-focusing [8] give rise to stimulated scattering processes [9–11]. The scattered light can be amplified to a high power level which then reduces the laser intensity in the medium [12, 13]. Since the self-focusing action depends critically on the laser light intensity, it is influenced strongly by stimulated scattering processes [12].

Previous quantitative investigations concentrated on self-focusing length and threshold power [14–16].

Reprints request to Dr. M. MAIER, Physik-Department E 11 der Technischen Universität München, Arcisstraße 21.

* New address: Messerschmitt-Bölkow-Blohm GmbH (KN 15), 8 München, Landwehrstr. 73.

[1] G. A. ASKAR'YAN, Sov. Phys. JETP **15**, 1088 [1962]. — V. I. TALANOV, Izv. Vysshikh Uchebn. Zavedenii Radiofiz. **7**, 564 [1964].

[2] R. Y. CHIAO, E. GARMIRE, and C. H. TOWNES, Phys. Rev. Letters **13**, 479 [1964].

[3] S. A. AKHMANOV, A. P. SUKHORUKOV, and R. V. KHOKHLOV, Sov. Phys. Uspekhi **93**, 609 [1968].

[4] V. N. LUGOVOI and A. M. PROKHOROV, JETP Letters **7**, 117 [1968]. — M. M. T. LOY and Y. R. SHEN, Phys. Rev. Letters **22**, 994 [1969].

[5] M. M. DENARIEZ-ROBERGE and J.-P. TARAN, Appl. Phys. Letters **14**, 205 [1969].

[6] N. F. PILIPETSKII and A. R. RUSTAMOV, JETP Letters **2**, 55 [1965]. — R. Y. CHIAO, M. A. JOHNSON, S. KRINSKY, H. A. SMITH, C. H. TOWNES, and E. GARMIRE, IEEE J. Quantum Electr. **2**, 467 [1966]. — D. H. CLOSE, C. R. GIULIANO, R. W. HELLWARTH, L. D. HESS, F. J. MCCLUNG, and W. G. WAGNER, IEEE J. Quantum Electr. **2**, 553 [1966]. — E. GARMIRE, R. Y. CHIAO, and C. H. TOWNES, Phys. Rev. Letters **16**, 347 [1966]. — R. G. BREWER and J. R. LIFSHITZ, Phys. Letters **23**, 79 [1966]. — R. G. BREWER and C. H. TOWNES, Phys. Rev. Letters **18**, 196 [1967]. — S. SAIKAN and H. TAKUMA, IEEE J. Quantum Electr. **4**, 618 [1968]. — R. G. BREWER, J. R. LIFSHITZ, E. GARMIRE, R. Y. CHIAO, and C. H. TOWNES, Phys. Rev. **166**, 326 [1968]. — F. SHIMIZU and B. P. STOICHEFF, IEEE J. Quantum Electr. **5**, 544 [1969].

[7] G. L. MCALLISTER, J. H. MARBURGER, and L. G. DESHAZER, Phys. Rev. Letters **21**, 1648 [1968].

[8] G. HAUCHECORNE and G. MAYER, C. R. Acad. Sci. Paris **261**, 4014 [1965]. — Y. R. SHEN and Y. J. SHAHAM, Phys. Rev. Letters **15**, 1008 [1965]. — P. LALLEMAND and N. BLOEMBERGEN, Phys. Rev. Letters **15**, 1010 [1965].

[9] N. BLOEMBERGEN, Nonlinear Optics, W. A. Benjamin, New York 1965; Amer. J. Phys. **35**, 989 [1967].

[10] W. KAISER and M. MAIER, Stimulated Rayleigh, Brillouin and Raman Spectroscopy; Laser Handbook, to be published.

[11] M. MAIER, O. RAHN, and H. J. NEUSSER, Self-Focusing of Laser Light and Stimulated Scattering Processes: 2. Stimulated Raman and Brillouin Scattering; to be published.

[12] M. MAIER, G. WENDL, and W. KAISER, Phys. Rev. Letters **24**, 352 [1970].

[13] M. MAIER, W. KAISER, and J. A. GIORDMAINE, Phys. Rev. **177**, 580 [1969].

[14] C. C. WANG, Phys. Rev. Letters **16**, 344 [1966].

[15] M. MAIER and W. KAISER, Phys. Letters **21**, 529 [1966]. — N. BLOEMBERGEN, P. LALLEMAND, and A. PINE, IEEE J. Quantum Electr. **2**, 246 [1966].

[16] C. C. WANG, Phys. Rev. **152**, 149 [1966]. — Y. R. SHEN and Y. J. SHAHAM, Phys. Rev. **163**, 224 [1967].

No information on the spatial development of the self-focusing process was given. In these papers the onset of stimulated Raman scattering was taken as an indication for the occurrence of self-focusing action. The self-focusing length was measured as a function of incident laser power for different substances, and good agreement with theory was found [14]. Measurements of the threshold power as a function of the nonlinearity of the refractive index in liquids were also in accordance with theoretical calculations [15].

This paper presents detailed investigations of the spatial and temporal development of the self-focusing process. Experiments are performed in transparent and absorbing liquids and compared quantitatively with theory. In Sec. II, numerical solutions of the wave equation are given for the case of self-focusing of divergent light beams. Problems concerning the comparison between experiments and theory are discussed in Sec. III, followed by a description of the experimental apparatus in Sec. IV. The experimental results are treated in Sec. V and summarized in Sec. VI.

II. Theory of Self-Focusing of Light

The propagation of light in a medium is described by Maxwells equations, which lead to the wave equation [2] for the electric field $\boldsymbol{E}$

$$\nabla^2\boldsymbol{E} - \frac{\varepsilon_0}{c^2}\frac{\partial^2\boldsymbol{E}}{\partial t^2} - \frac{\sqrt{\varepsilon_0}\,\alpha}{c}\frac{\partial\boldsymbol{E}}{\partial t} - \frac{\varepsilon_2}{c^2}\frac{\partial^2(E^2\boldsymbol{E})}{\partial t^2} = 0\,. \qquad (1)$$

Here α is the absorption coefficient and c the velocity of light in vacuum. In Eq. (1), the dielectric constant ε was assumed to depend on the electric field as

$$\varepsilon = \varepsilon_0 + \varepsilon_2 E^2\,. \qquad (2)$$

Since, in the present paper, self-focusing action is investigated only in the region of relatively large diameters and correspondingly low intensities, it is justified to neglect higher terms in the expansion of ε. The measurements are made in CS_2 and molten para-di-chlorobenzene, both liquids having molecules with highly anisotropic polarizability. In these liquids the major contribution to the nonlinearity of the dielectric constant comes from the optical Kerr effect. ε_2 can be calculated from the Kerr constant [17]. The following numbers are used [18, 19]: CS_2, $\varepsilon_2 = 4.2\times10^{-11}$ cm^3/erg; para-di-chlorobenzene ($T = 70$ °C), $\varepsilon_2 = 2.9\times10^{-11}$ cm^3/erg.

In solving the wave equation (1) linearly polarized plane waves with slowly varying amplitudes are considered. In the experiments we use light pulses which are long (~ 500 cm) compared to the length of the nonlinear medium (~ 30 cm). In addition, these pulses are long compared to the relaxation time of the Kerr effect [20]. The assumption of a quasi steady-state in the self-focusing action is a good approximation. By introducing normalized cylindrical coordinates with radial distance $\bar{r} = r/a$, axial distance $\bar{z} = z/2\,k_L\,a^2$, absorption coefficient $\bar{\alpha} = 2\,k_L\,a^2\,\alpha$, and electric field $\bar{E}_L = (\varepsilon_2/2\,\varepsilon_0)^{1/2}\,k_L\,a\,E_L = 2\,k_L(P_L\,\varepsilon_2/c\,\varepsilon_0^{3/2})^{1/2}$, we obtain [21, 22]

$$i\frac{\partial\bar{E}_L}{\partial\bar{z}} + \frac{\partial^2\bar{E}_L}{\partial\bar{r}^2} + \frac{1}{\bar{r}}\frac{\partial\bar{E}_L}{\partial\bar{r}} + \frac{i\,\bar{\alpha}}{2}\bar{E}_L + |\bar{E}_L|^2\bar{E}_L = 0\,. \qquad (3)$$

Here a is the 1/e radius of the Gaussian intensity distribution of the incoming beam (see below), E_L and P_L are the amplitude of the laser field and the laser power, respectively, and $k_L = \sqrt{\varepsilon_0}\,\omega_L/c$ is the wave vector. Equation (3) is transformed into a difference equation [21, 22], which is solved numerically with a computer for the following experimental situation:

A light beam characterized by a power, by an intensity distribution over the cross section, by a beam diameter and a divergence is incident on a medium of length l (see Fig. 1). The initial conditions of the calculations are given by the properties of the light beam at the entrance of the medium ($z = 0$). We are interested in the intensity distribution at the end of the medium ($z = l$). So far parallel incident light beams have been treated in the literature [21–25] in most cases. In our calculations the

[17] For linearly polarized light $\varepsilon_2 = (4/3)\,\sqrt{\varepsilon_0}\,\lambda\,B$. λ is the wavelength of light, B the optical Kerr constant.

[18] M. Paillette, C. R. Acad. Sci. Paris **262**, 264 [1966].

[19] Landolt-Börnstein, Zahlenwerte und Funktionen aus Physik, Chemie, Astronomie, Geophysik und Technik (Springer-Verlag, Berlin 1962), Vol. II, Pt. 8.

[20] The relaxation time of the orientation Kerr effect in CS_2 is 2 psec; S. L. Shapiro and H. P. Broida, Phys. Rev. **154**, 129 [1967].

[21] P. L. Kelley, Phys. Rev. Letters **15**, 1015 [1965].

[22] E. L. Dawes and J. H. Marburger, Phys. Rev. **179**, 862 [1969].

[23] A. L. Dyshko, V. N. Lugovoi, and A. M. Prokhorov, JETP Letters **6**, 146 [1967].

[24] J. H. Marburger and E. Dawes, Phys. Rev. Letters **21**, 556 [1968].

[25] V. N. Goldberg, V. I. Talanov, and R. W. Erm, Izv. Vysshikh Uchebn. Zavedenii Radiofiz. **10**, 674 [1967].

effect of beam divergence is fully taken into account because of its strong influence on the self-focusing process. The laser beam is represented by a spherical wave diverging from point $z=-R$ (see Fig. 1).

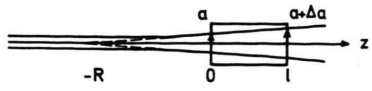

Fig. 1. The divergent laser beam is approximated by a spherical wave originating from point $z=-R$. a and $a+\Delta a$ are the $1/e$ radii at $z=0$ and $z=l$, respectively.

This is a good approximation in our experiments since the distance between the laser and the liquid cell is large. Assuming a Gaussian intensity distribution over the cross section (as was measured in the experiments), we introduce the complex amplitude of a spherical wave

$$E_L = \frac{E_M}{1+z/R} \exp\left\{ -\frac{r^2}{2\,a^2(1+z/R)^2} - i\,k_L \frac{r^2}{2(z+R)} \right\}. \tag{4}$$

If no self-focusing occurs, the quantity R is determined from the $1/e$ radius at the entrace (a) and at the end $(a+\Delta a)$ of the medium (see Fig. 1). R is given by $a\,l/\Delta a$. Equation (4) yields the complex amplitude at $z=0$

$$E_L(z=0) = E_M\, e^{-r^2/2a^2}\{\cos(k_L\, r^2\, D\,V/2\,a) + i\,\sin(k_L\, r^2\, D\,V/2\,a)\}. \tag{5}$$

The beam divergence is defined as $D\,V=\Delta a/l$, with the normalized value $\overline{D\,V}=D\,V(k_L\,a/2)=\Delta a/4\,\bar{l}$. For a convergent, parallel, or divergent light beam Δa is negative, zero, or positive, respectively.

Using the initial conditions of our experiments, Eq. (3) has been solved numerically for self-focusing in transparent as well as absorbing media. A comparison with experimental results will be made in Sec. V.

1. *Transparent Media*

As a typical example for self-focusing in transparent media Fig. 2 shows the calculated intensity distributions at different distances z in CS_2. The incident light beam is assumed to have a Gaussian intensity distribution with a diameter of 435 μ, a power of $P_L=100$ kW and a divergence of $D\,V=5\times10^{-4}$ rad (in the medium). The absorption of pure CS_2 is neglected because it is very small ($\alpha\cong10^{-3}\,\mathrm{cm}^{-1}$). In transparent media self-focusing has the following characteristic properties: there is a drastic reduction of beam diameter and a strong increase of on-axis intensity (see Fig. 2). This type of self-focusing is sometimes called catastrophic focusing.

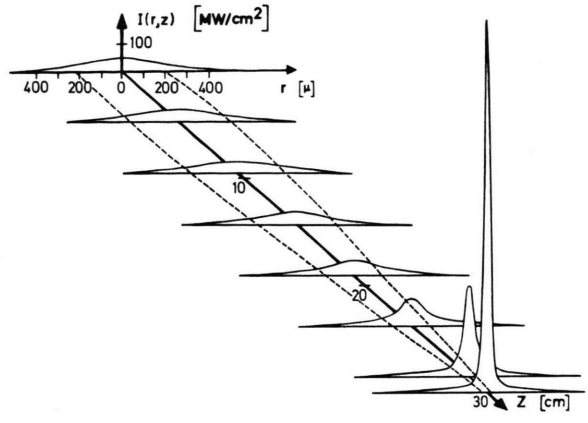

Fig. 2. Propagation of an intense light beam through CS_2 (cell length $l=30$ cm). Gaussian intensity distribution at $z=0$ with a diameter $d_0=435$ μ, laser power $P_L=100$ kW, beam divergence $D\,V=5\times10^{-4}$ rad (in CS_2). The dotted line shows the dependence of the beam diameter on z.

In the following figures the normalized quantities introduced above are used at the lower scale. The numbers at the upper scale and in brackets correspond to a light beam of wavelength $\lambda_L=6943$ Å with a $1/e$ radius $a=261$ μ incident on CS_2.

In Fig. 3 the intensity distributions at different distances z are redrawn from Fig. 2 to show that strong variations are found. It is important to notice

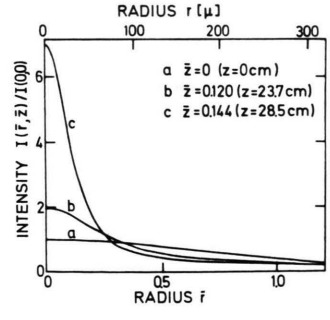

Fig.3. Intensity $I(\bar{r},\bar{z})/I(0,0)$ versus radial distance $\bar{r}$ at different distances in CS_2 (taken from Fig. 2).

that drastic intensity changes occur in the center of the beam, while the outer portions of the beam experience smaller changes. The result is compared with the experiments in Sec. V, 1 a.

The examples shown in Fig. 4 demonstrate the strong influence of beam divergence on self-focusing

action. In Figs. 4 a and b the normalized on-axis intensity $I_M(\bar{z})/I_M(0)$ and the corresponding normalized diameter $\bar{d}$ are plotted as a function of distance $\bar{z}$. Curves 1 show the self-focusing of a

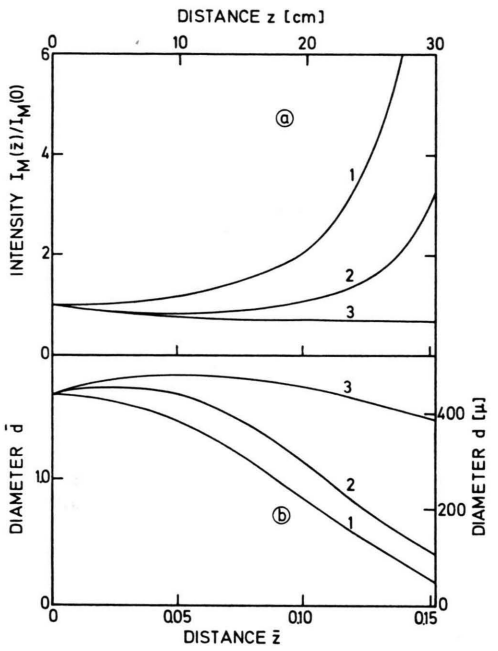

Fig. 4. a) Normalized on-axis intensity $I_M(\bar{z})/I_M(0)$ and b) normalized beam diameter $\bar{d}$ versus normalized distance $\bar{z}$. 1) Normalized field $\bar{E}_L = 3.8$ ($P_L = 51$ kW), normalized divergence $\overline{DV} = 0$; 2) $\bar{E}_L = 5.0$ ($P_L = 89$ kW), $\overline{DV}=1$ ($DV=5\times10^{-4}$ rad); 3) $\bar{E}_L=3.8$ ($P_L=51$ kW), $\overline{DV}=1$ ($DV=5\times10^{-4}$ rad). The numbers in ordinary units correspond to a light beam of wavelength $\lambda_L=6943$ Å and $1/e$ radius $a=261$ μ in CS_2.

parallel light beam ($DV=0$) with $\bar{E}_L=3.8$ ($P_L=51$ kW). Curves 2 and 3 correspond to divergent light beams $\overline{DV}=1$ ($DV=5\times10^{-4}$ rad) with $\bar{E}_L=5.0$ and 3.8, respectively ($P_L=89$ and 51 kW). A comparison between curves 1 and 3 demonstrates clearly the striking influence of the beam divergence on the self-focusing action. With increasing divergence self-focusing is reduced. For a divergent beam more power is needed (curve 2) than for a parallel beam (curve 1) in order to get a strong increase of intensity and reduction of beam diameter.

2. *Absorbing Media*

Because of the strong intensity dependence of self-focusing a reduction of this effect is expected in lossy substances where part of the laser power is absorbed. Figure 5 shows a typical example of our numerical calculations. The normalized on-axis intensity is plotted as a function of normalized distance $\bar{z}$ for relatively high absorption ($\alpha l=4$) and a laser field $\bar{E}_L=9.2$ ($P_L=300$ kW) with a divergence $\overline{DV}=1.0$ ($DV=5\times10^{-4}$ rad in the medium). The solid line represents a nonlinear

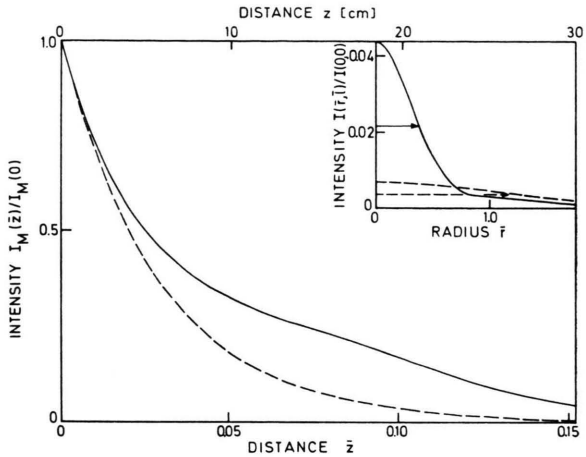

Fig. 5. On-axis intensity $I_M(\bar{z})/I_M(0)$ versus distance $\bar{z}$ in an absorbing medium ($\alpha l=4$, $\bar{E}_L=9.2$, $\overline{DV}=1.0$). The insert shows the intensity distribution at the end of the medium ($\bar{l}=0.1518$). The solid and broken lines correspond to a nonlinear ($\varepsilon_2 \neq 0$) and linear ($\varepsilon_2=0$) medium, respectively.

medium, the broken line a linear medium, where no self-focusing occurs. A comparison between these curves shows clearly the increase of on-axis intensity due to self-focusing. The intensity distribution at the end of the medium $\bar{l}=0.1518$ ($l=30$ cm) is given in the inset. It is evident that even in strongly absorbing media the beam diameter is reduced drastically by self-focusing. This type of self-focusing where, even for decreasing on-axis intensity, a reduced beam diameter is observed will be called weak focusing.

Figure 6 shows self-focusing in absorbing media for different incident laser powers. The divergence of the laser beam is $\overline{DV}=1$, the absorption is $\alpha l=4$. In Fig. 6 a the normalized intensity in the center of the beam $I_M(\bar{z})/I_M(0)$ is plotted as a function of distance $\bar{z}$. At small laser power (1) $\bar{E}_L=5.3$ ($P_L=100$ kW) $I_M(\bar{z})$ decreases monotonously. At higher power values (2) $\bar{E}_L=10.6$ ($P_L=400$ kW) a maximum is obtained where the self-focusing action is balanced by the absorption. It is seen from Fig. 6 b that even for decreasing on-axis intensity a reduction of beam diameter is observed due to self-focusing. A catastrophic focus is found only for

high incident laser powers (3) $\bar{E}_L = 11.23$ ($P_L =$ 450 kW). Here, the on-axis intensity increases drastically, similar to the case of transparent media. These results compare well with those of Refs. 22 and 25 which were obtained for different initial conditions.

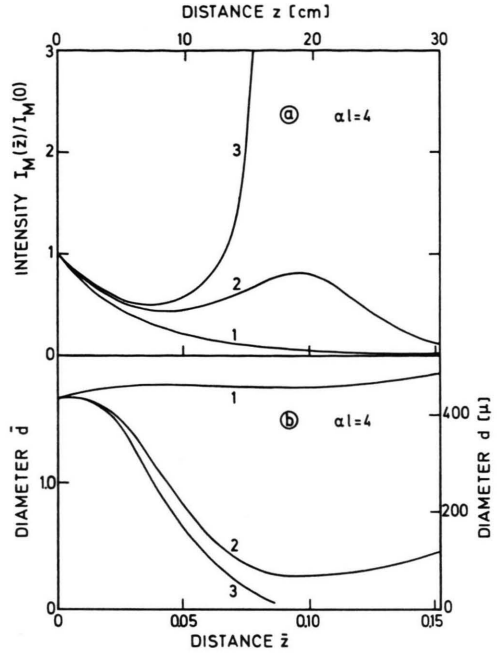

Fig. 6. a) On-axis intensity $I_M(\bar{z})/I_M(0)$ versus distance $\bar{z}$, b) diameter $\bar{d}$ versus $\bar{z}$ in an absorbing medium ($\alpha l = 4$, $\overline{DV} = 1$). 1) $\bar{E}_L = 5.3$ ($P_L = 100$ kW); 2) $\bar{E}_L = 10.6$ ($P_L = 400$ kW); 3) $\bar{E}_L = 11.23$ ($P_L = 450$ kW).

The numerical calculations described above show that even in strongly absorbing liquids self-focusing of light plays an important role if the incident laser power is high enough.

III. Comparison between Theory and Experiments

As shown in the preceding section, on-axis intensities and intensity distributions over the cross section are readily calculated from theory. However, experimentally power and energy values are measured instead of intensities. Photocells determine the integral of the intensity over the beam area, i.e. the power; photographic plates measure the integral of the intensity over the time, i.e. the energy per cm^2. For a quantitative comparison with experiments the theoretical results have to be integrated over time or beam area.

The integration over time was done by approximating the laser pulse with rectangles of width Δt_i (see Fig. 7). Assuming a quasi steady-state behavior[20] of the self-focusing process, the intensity distribution $I_i(r)$ at the end of the medium was calculated for each rectangle. The total energy density is obtained as the sum over the individual contributions $D(r) \cong \sum_i I_i(r)\, \Delta t_i$. This value will be compared directly with the measured curves in Sec. V,1.

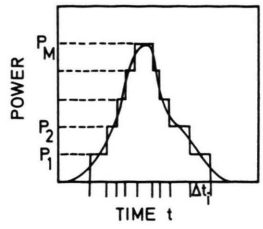

Fig. 7. Approximation of the laser pulse by rectangles for the numerical integration of the intensity distribution over time t.

Time-resolved measurements of self-focusing are described in detail in Sec. V,2 (see also Fig. 14). Part of the transmitted light in the center of the beam is coupled out by a mirror. Its power P_c is measured with a fast photocell and an oscilloscope. For a comparison between theory and experiments the intensity distribution at the end of the medium is calculated for different incident laser powers and integrated over the area of the mirror (radius r_c). The result is shown in Fig. 8. The light beam has a divergence of $\overline{DV} = 1.0$ ($DV = 5 \times 10^{-4}$ rad), the length of the medium is $\bar{l} = 0.1518$ ($l = 30$ cm), the radius of the mirror is $\bar{r}_c = 0.368$ ($r_c = 95\,\mu$). The

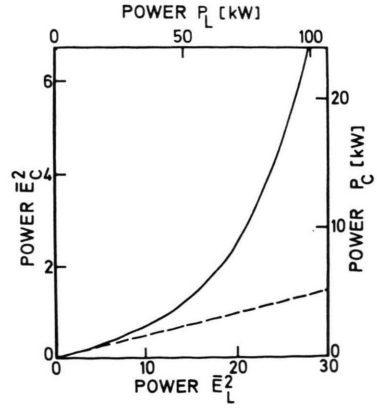

Fig. 8. Normalized power $\bar{E}_c^2$ in the center of the beam versus normalized incident laser power $\bar{E}_L^2$ for a nonlinear (solid curve) and a linear (broken curve) medium. Beam divergence $\overline{DV} = 1$ ($DV = 5 \times 10^{-4}$ rad), length of the medium $\bar{l} = 0.1518$ ($l = 30$ cm).

normalized power $\bar{E}_c^2 \sim P_c$ in the center of the beam increases nonlinearly with the laser power $\bar{E}_L^2 \sim P_L$. In a non self-focusing medium $\bar{E}_c^2$ rises linearly (see broken line in Fig. 8).

Using Fig. 8 it is possible to predict P_c as a function of time, if the time dependence of the laser power P_L is known and a quasi steady-state behavior is assumed. In Sec. V,2 the theoretical results are compared with the experiments.

IV. Experimental

For the experimental investigations a giant-pulse ruby laser with a plane resonator was employed. Transverse and longitudinal mode selection was obtained by using a diaphragm in the resonator and a Fabry-Perot etalon as the front mirror. The laser emitted light of a single frequency with a spectral width of less than 0.01 cm^{-1}. The intensity distribution over the cross section was nearly Gaussian. The peak power was 500 kW and the pulse duration was 15 – 20 nsec. The laser light was linearly polarized and had a divergence $DV = 3 \times 10^{-4}$ rad.

The light power was measured with fast photocells and oscilloscopes (risetime $\cong 0.3$ nsec). The photocells were calibrated with a laser calorimeter [26]. The accuracy of the measurements of the absolute power values was approximately 20%.

V. Experimental Results and Discussion

Most of the papers on self-focusing are concerned with the region of limiting diameters [6, 27]. Because of the high intensity (> 10 GW/cm^2) in this region stimulated scattering processes occur. The interaction between self-focusing and stimulated scattering processes is quite complicated. It is difficult to get quantitative information on this region. On the other hand, a quantitative comparison between theory and experiment is obtained more readily in the region of relatively large diameters. Our experiments are confined to this region. They were performed in transparent and absorbing liquids under widely varying experimental conditions.

1. Photographic Investigations of Self-Focusing

The experimental set up is shown schematically in Fig. 9. The distance between the giant pulse ruby laser and the liquid cell is large in order to avoid multiple stimulated Brillouin scattering [28]. The beam diameter (full width at half maximum intensity) is reduced by an inverted telescope to $d_0 = 435\,\mu$ at the entrance window of the liquid cell. The beam

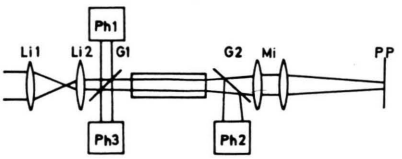

Fig. 9. Schematic of experimental system for measuring the intensity distribution of the light beam at the exit window of the liquid cell. Microscope Mi produces a magnified image of the exit window of the liquid cell on the photographic plate PP. G1, G2 glass plates; Ph1, Ph2, Ph3 fast photocells.

divergence after the telescope was $DV = 8 \times 10^{-4}$ rad (in air). The measurements were made with liquid CS_2 (length 30 cm) and molten para-dichlorobenzene ($T = 70\,^\circ$C; cell length 40 cm). A microscope Mi produced a magnified image of the exit window on the photographic plate PP (Kodak I-N). Glass plates G 1 and G 2 served to couple out a small amount of the incident laser light P_L (Phl), the backward scattered light (Ph 3) and the total transmitted laser light P_T (Ph 2). All signals were measured with fast photocells and oscilloscopes. The incident laser power was variied from shot to shot by a short absorption cell ($CoCl_2$ in ethanol). At the maximum laser power used in the experiments no thermal blooming [29] or stimulated thermal Rayleigh scattering [30] occured in this cell. Diameter and divergence of the beam remained unchanged after passage through the cell.

[26] We would like to thank Dr. HILLENKAMP for lending us his laser calorimeter.

[27] A. V. BUTENIN, V. V. KOROBKIN, A. A. MALYUTIN, and M. YA. SHCHELEV, JETP Letters **6**, 173 [1967]. — V. V. KOROBKIN and R. V. SEROV, JETP Letters **6**, 135 [1967].

[28] M. MAIER, Phys. Rev. **166**, 113 [1968].

[29] R. L. CARMAN and P. L. KELLEY, Appl. Phys. Letters **12**, 241 [1968]. — S. A. AKHMANOV, D. P. KRINDACH, A. V. MIGULIN, A. P. SUKHORUKOV, and R. V. KHOKHLOV, IEEE J. Quantum Electr. **4**, 568 [1968].

[30] R. M. HERMAN and M. A. GRAY, Phys. Rev. Letters **19**, 824 [1967]. — D. H. RANK, C. W. CHO, N. D. FOLTZ, and T. A. WIGGINS, Phys. Rev. Letters **19**, 828 [1967]. — W. ROTHER, H. MEYER, and W. KAISER, Z. Naturforsch. **25 a**, 1136 [1970].

a) Intensity Distribution of the Self-Focused Light

We determined the time-integrated intensity distribution of the laser beam at the exit window of the liquid cell. Near-field photographs were taken for different incident laser powers P_L. After calibrating the photographic plate with laser light, the time-integrated intensity distributions (or energy density distributions) were determined from microdensitometer traces.

In Fig. 10 a and b two examples are shown for CS_2. For a maximum transmitted laser power of $P_T^{max} = 51$ kW self-focusing is very weak. In striking contrast a drastic reduction of beam diameter and an increase of on-axis intensity occurs for $P_T^{max} = 89$ kW. The solid lines represent the microdensitometer curves (they are in the linear range of the density curve of the photographic plate), the broken lines are determined by numerical calculations. Both curves are adjusted at the maximum. Since the photographic plate integrates over time, comparison is made with the calculated time-integrated curves as obtained in Sec. III. There is good agreement between both curves.

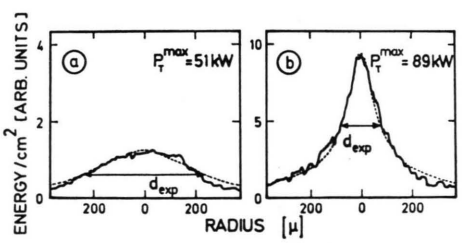

Fig. 10. Distribution of the energy density at the exit window of the liquid cell filled with CS_2; microdensitometer traces (solid lines) and calculated curves (broken lines). a) Maximum transmitted power $P_T^{max} = 51$ kW; b) $P_T^{max} = 89$ kW. Note that different ordinates were used in a) and b).

The experimental distributions at the exit window strongly deviate from a Gaussian, in agreement with theory. It should be noticed that focusing occurs mainly in the center of the beam, while the outer part is affected to a less extent.

b) Dependence of Beam Diameter on Laser Power

With the intensity distribution over the cross section of the beam obtained in the preceding section the beam diameter d_{exp} at the exit window was determined with an accuracy of approximately 20% (see Fig. 10). The intensity distribution, the incident (P_L) and transmitted (P_T) laser power, the backward scattered Raman (P_R) and Brillouin (P_B) power were measured simultaneously for each laser pulse. In Figs. 11 a and b the beam diameter d (open circles) is plotted as a function of the maximum transmitted laser power P_T^{max} for CS_2 and molten para-di-chlorobenzene. It will be apparent in Sec. V,2 that the maximum transmitted laser power P_T^{max} not the maximum incident laser power P_L^{max} is the determining parameter for the occurrence of self-focusing. The solid line d_{cal} was calculated with a computer (see Sec. II.1) considering the initial conditions (beam diameter $d_0 = 435\ \mu$ and divergence $DV = 5 \times 10^{-4}$ rad in CS_2). At small power values (no self-focusing) the beam diameter at the end of the cell is $\sim 700\ \mu$ because of the finite beam divergence. The experimental points represent time-integrated values. The broken lines show the beam diameters d_{int} obtained from the time integration discussed in Sec. III. In the following sections we compare experimental results with calculated curves which were not integrated over time, since there is only a small difference between d_{cal} and d_{int} in Fig. 11.

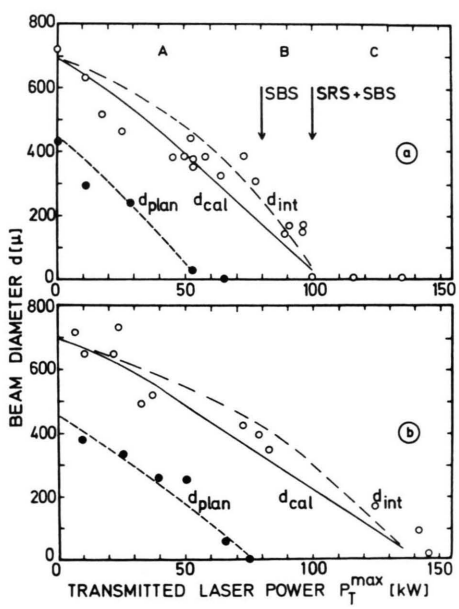

Fig. 11. Beam diameter d at the exit window as a function of the maximum transmitted laser power P_T^{max}. The experimental points correspond to a parallel (●) and divergent (○) light beam. a) CS_2; b) molten para-di-chlorobenzene ($T = 70$ °C). The three curves for d_{plan}, d_{cal}, and d_{int} are calculated; for details see text.

Next, the effect of a reduction of beam divergence on self-focusing will be discussed. The distance between lenses Li 1 and Li 2 of the telescope in Fig. 9 was equal to the sum of their focusing lengths. When this distance is slightly increased the beam divergence is reduced. It is possible to have the beam diameter approximately constant along the length of the (empty) cell. Self-focusing was investigated with this "parallel" beam. The diameter at the exit window was measured as a function of laser power. The experimental points (●) are shown in Fig. 11 together with the calculated curves d_{plan} (dotted lines) where plane waves were used as initial conditions ($d_0 = 435\ \mu$, $DV = 0$).

The agreement between the experimental points and the calculated curves is good in CS_2 and para-di-chlorobenzene both for divergent and "parallel" incident light. It should be noted that no fitting parameters were used in Fig. 11. Each experimental point corresponds to a single laser pulse; there was no averaging over many laser pulses. In agreement with theory, the experimental results show clearly that self-focusing of light is very sensitive to changes of beam divergence as well as to the nonlinearity of refractive index. For a parallel beam the laser power necessary to obtain the minimum diameter of 5 μ is smaller by a factor of approximately 2 compared to that of a divergent beam ($DV = 5 \times 10^{-4}$ rad in CS_2). This power level is lower in CS_2 than in para-di-chlorobenzene because of the higher nonlinearity of refractive index in CS_2 (see Sec. II)[31].

For each laser pulse stimulated Brillouin scattering (SBS) and stimulated Raman scattering (SRS) in the backward direction were measured simultaneously with the beam diameter. Three different regions A, B, and C can be distinguished in Fig. 11 a for CS_2. We discuss here the divergent beam, but similar results are obtained for the parallel beam.

A) At moderate laser power levels, $P_T^{max} < 80$ kW, no stimulated scattering processes are observed, i.e. their power values are below the sensitivity of the fast detection system.

B) At an intermediate power range, only SBS is seen. From additional experiments[11] (where a photomultiplier was used) we know that SRS occurs. The power values are too low for detection with the fast photocells used in the present investigations.

C) At high laser power, $P_T^{max} > 100$ kW, SRS in the forward and backward direction and subsequently SBS is observed. The onset of these processes is discussed in detail in Ref. [11]. Our computer calculations of the self-focusing action are not applicable in that power range since the processes limiting the beam diameter are not known. In addition, the interaction of laser light with the scattered light was not considered in our calculations.

In para-di-chlorobenzene SRS and SBS were seen only in the region of limiting diameter 5 μ ($P_T^{max} > 140$ kW for divergent laser light, $P_T^{max} > 70$ kW for a parallel beam, see Fig. 11 b).

c) Beam Diameter in Absorbing CS_2

The experimental set up for the investigation of the beam diameter in absorbing CS_2 is the same as in Fig. 9. The intensity distributions and beam diameters are determined from microdensitometer traces of the photographic plates. We investigated solutions of iodine in CS_2 with different absorption coefficient α. The length of the liquid cell was $l = 30$ cm, the beam divergence $DV = 5 \times 10^{-4}$ rad (in CS_2) and the diameter $d_0 = 435\ \mu$.

In Fig. 12 the beam diameter d at the exit window is plotted as a function of maximum transmitted laser power $P_T^{max}\, e^{\alpha l}$ for transparent CS_2 (○) and CS_2: I_2 (●). The absorption was relatively large $\alpha l = 4$, i.e. the power transmission of the cell was only 2%. The solid curves were calculated according to Sec. II for the initial values given above. The

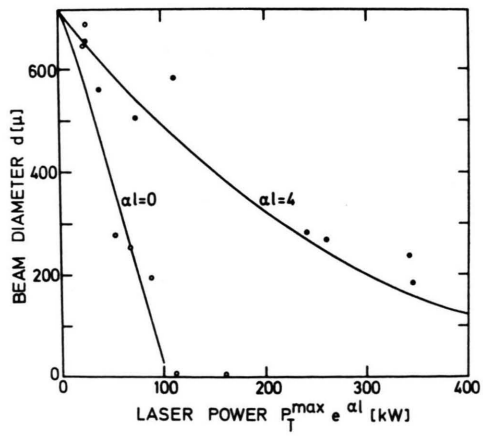

Fig. 12. Beam diameter d as a function of laser power $P_{T\max}\, e^{\alpha l}$ in transparent (○) and absorbing (●) CS_2. The solid curves are calculated.

[31] From a comparison with our computer calculations it is seen that the dependence of self-focusing action on beam divergence and nonlinearity of refractive index is described qualitatively by the approximate analytical solutions given e. g. in Ref. [3].

agreement between theory and experiments is quite good both for transparent and absorbing CS_2. It should be noted that experimentally a reduction of beam diameter up to a factor of 4 is observed inspite of the high absorption $\alpha l = 4$. This behavior is expected from theory as was discussed in Sec. II,2. SBS was observed only at the highest laser power (>450 kW); SRS was not detected with fast photocells.

The reduction of the self-focusing action expected for increasing absorption was checked by measuring the beam diameter as a function of absorption αl at constant incident laser power. A laser power of 100 kW was used, since no stimulated scattering processes occured in the entire absorption range at this power value. It should be noted that the incident beam diameter ($d_0 = 590\ \mu$) in this measurement was larger than usual ($d_0 = 435\ \mu$) while the divergence was smaller, $DV = 3.6 \times 10^{-4}$ rad in CS_2. Stimulated scattering processes could only be observed at laser powers in excess of 100 kW.

Within the experimental accuracy of approximately 20% the measured points (○) shown in Fig. 13 are in good agreement with the numerical calculations (solid curve). It is clearly evident that the beam diameter increases from 300 μ to 600 μ when the absorption is increased to $\alpha l = 7$ [32].

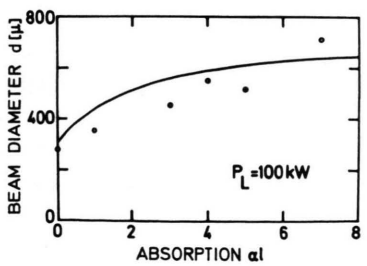

Fig. 13. Beam diameter d versus absorption αl in CS_2 at constant incident laser power P_L (see text). The solid curve is calculated numerically.

[32] We investigated the beam diameter at the exit window of a cell filled with CCl_4 coloured by small amounts of iodine, where self-focusing is of minor importance at the laser power used. No increase of beam diameter due to thermal blooming [29] or stimulated thermal Rayleigh scattering [30] was observed for an absorption $\alpha l = 4$ at our highest laser power. Since the material parameters relevant for these processes have similar values in CCl_4 and CS_2 we conclude that both effects are not important in absorbing CS_2. This conclusion is supported by the agreement between theory and experiments on self-focusing in absorbing CS_2. At higher laser power thermal blooming and stimulated thermal Rayleigh scattering are known to be present in absorbing CCl_4 (W. ROTHER and K. DARÉE, private communication).

2. *Time-Resolved Investigations of Self-Focusing*

No information on the time dependence of self-focusing is obtained from photographic investigations, since the photographic plate is a time-integrating device. It has been suggested [4, 13] that stimulated scattering processes influence strongly self-focusing of the laser beam. Our time-resolved measurements demonstrate the important role of SRS and SBS in a very direct way.

The experimental set up for measuring the time dependence of self-focusing is shown in Fig. 14. It is similar to the apparatus of Fig. 9, with the photographic plate PP replaced by a mirror S with a diameter of 2.5 mm. A microscope Mi produces a magnified image of the exit window at mirror S. At a magnification of 13, the diameter of the mirror

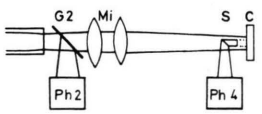

Fig. 14. Schematic of the experimental system for measuring the time evolution of self-focusing action. The exit window of the liquid cell is imaged through a microscope Mi to mirror S. G2 glass plate; Ph2, Ph4 fast photocells; C camera.

corresponds to 190 μ at the exit window. The mirror only reflects the power in the center of the beam to photocell 4. The relative position of the laser beam and mirror S is controlled at each laser pulse by taking pictures with camera C. Photocell 4 measures the transmitted laser power P_c within a diameter of 190 μ. With increasing laser power self-focusing increases, i.e. more light is concentrated into the center of the beam (see Fig. 10). Signal P_c is, therefore, a measure of self-focusing action; it increases nonlinearly with laser power. The total time resolution of Ph 4 and oscilloscope was 0.5 nsec. The beam diameter at the entrance window was $d_0 = 435\ \mu$, the divergence was $DV = 5 \times 10^{-4}$ rad in CS_2.

a) Transparent CS_2

In Fig. 15 three typical examples of the time dependence of self-focusing in CS_2 are shown for three different laser powers. Fig. 15 a shows oscilloscope traces of the incident laser power P_L, the total transmitted power P_T and the signal P_c from photocell 4. In Fig. 15 b the Brillouin power P_B and the Raman power P_R in the backward direction are depicted. All signals were measured simultane-

ously at one laser pulse. The three examples correspond to regions A, B and C in Fig. 11 a.

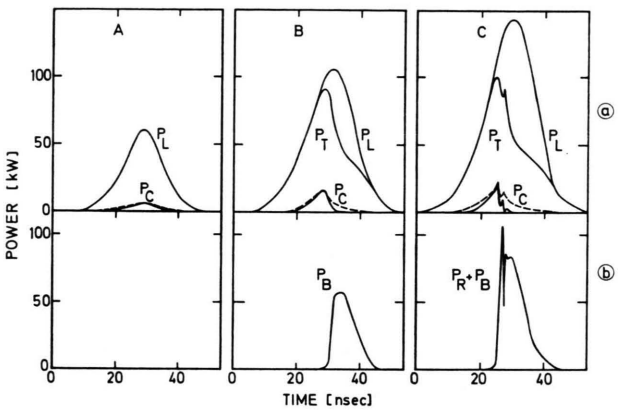

Fig. 15. a) Oscilloscope traces (redrawn) of the incident (P_L) and transmitted (P_T) laser power, and the central part of the transmitted power (P_C), a measure of self-focusing action in transparent CS_2. The broken lines are calculated. b) Backward stimulated Raman and Brillouin power P_R and P_B, respectively. A, B, and C correspond to three different laser powers.

A) No stimulated scattering processes were observed. Signal P_c depends nonlinearly on laser power, indicating a strong variation of beam diameter around the maximum of the laser pulse. Pulse sharpening in the center of the beam is observed [7, 33].

B) Stimulated Brillouin scattering occurred. In this region signal P_c increases in analogy to region A; a sudden decrease occurs when SBS is observed. Since P_c is a measure of the self-focusing action, the rapid decrease indicates a strong suppression of self-focusing by SBS.

C) Stimulated Raman and Brillouin scattering in the backward direction were observed. Signal P_c exhibits an abrupt break whenever SRS in the backward direction appears. SBS follows SRS inhibiting further self-focusing action.

The experimental results are compared with numerical calculations. Using the measured laser power, beam diameter and divergence at the entrance window, we made machine calculations to obtain the power P_c reflected via mirror S as a function of instantaneous incident laser power (see Sect. III). The theoretical curves (broken lines) are in good agreement with the measured power values P_c (solid lines) as long as no stimulated scattering processes occur. It should be emphasized that no fitting parameters were used.

The experimental and theoretical data yield the following result: As the incident laser power rises self-focusing is found to increase, i.e. the beam diameter is reduced and light is concentrated into the center of the beam. With subsequent reduction of laser power the beam diameter widens again and the on-axis intensity decreases.

When strong SBS or SRS is observed, the laser power decreases along the length of the cell. In this case the *transmitted* laser power was used for the calculations instead of the *incident* laser power, since for strong stimulated backward scattering the conversion into scattered light occurs within the first few cm of the cell ($l = 30$ cm) [28]. We believe this to be a good approximation, because the laser power over the greater part of the cell is close to the small power level transmitted through the exit. It is seen from Fig. 15 that the transmitted laser power P_T, determining the self-focusing action is substantially below the incident laser power P_L when stimulated scattering processes occur; P_T does not reach the maximum incident power level. The onset of stimulated Raman and Brillouin scattering is determined both by the transient behavior of SBS in that power range and the influence of self-focusing action; it will be discussed in detail in Ref. [11]. The deviations of the calculated from the measured values of P_c can be attributed to the fact that stimulated scattering processes were not considered in detail in our calculations. In addition to the variation along the length of the cell, the intensity distribution over the cross section is changed by these processes. The conversion of laser light into scattered light takes place mainly in the center of the beam where the intensity is high. The curvature of the laser intensity distribution is reduced here causing a smaller self-focusing effect. Therefore, signal P_c which measures the power in the center of the beam decreases more rapidly than the calculated curve. It is difficult to evaluate these two factors quantitatively since this would require a solution of the coupled differential equations for self-focusing and stimulated scattering processes.

It is somewhat arbitrary to define a time duration of the self-focusing action, since self-focusing starts at a low laser power, increases and decreases again at the end of the pulse. An "experimental" time

[33] J. H. MARBURGER and W. G. WAGNER, IEEE J. Quantum Electr. **3**, 415 [1967]. — G. L. MCALLISTER and L. G. DE SHAZER, IEEE J. Quantum Electr. **5**, 357 [1969].

duration may be defined as the interval of time when the beam diameter at the exit window is smaller than a definite, measurable fraction of its value without self-focusing. It is seen from Fig. 15 that the self-focusing action lasts for several nsec, even for high laser power (C). Signal P_c is the transmitted power integrated over a diameter of 190 μ. Variations of the beam diameter d are readily seen as long as d is not small compared to 190 μ. Rapid changes of small beam diameters, however, are not observed with this method. The duration of the limiting diameter was found in additional experiments, where only the highly divergent light emitted from this region was measured with a fast photocell, to be <0.5 nsec, in agreement with previous measurements [4, 13].

b) Absorbing CS_2

We have carried out time-resolved measurements in absorbing CS_2 for $\alpha l = 2$. The results are similar to those described in the preceding section for transparent CS_2. Again three different regions can be distinguished: A) No stimulated scattering processes ($P_L < 150$ kW), B) only SBS, and C) SRS and SBS occur ($P_L > 210$ kW).

Fig. 16 shows oscilloscope traces of the incident (P_L) and transmitted ($P_T e^{\alpha l}$) laser power, signal $P_c e^{\alpha l}$ which is a measure of self-focusing action, and backward stimulated Raman and Brillouin power ($P_R + P_B$). No oscilloscope pictures are given for regions A and B since the results are very similar to transparent CS_2 (Fig. 15 A and B). It is clearly seen from Fig. 16 that signal P_c exhibits a break when SRS and SBS are observed indicating a suppression of self-focusing action by these processes. A comparison between transparent and absorbing CS_2 (Fig. 15 C and 16) shows only minor differences. Since the conversion into scattered light is smaller in absorbing CS_2, self-focusing is not suppressed completely. A comparison between the measured (solid line) and calculated (broken line) curves of signal P_c indicates again satisfactory agreement (see Fig. 16).

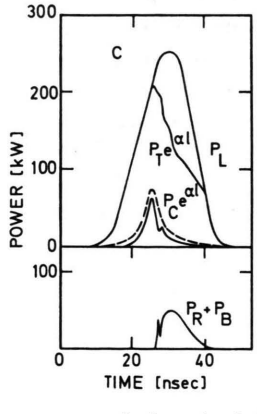

Fig. 16. Oscilloscope traces (redrawn) of the incident (P_L) and transmitted ($P_T e^{\alpha l}$) laser power, the central part of the transmitted power ($P_c e^{\alpha l}$), a measure of self-focusing action, and the backward stimulated Raman and Brillouin power (P_R and P_B) in absorbing CS_2 ($\alpha l = 2$). The broken line is calculated.

Our time-resolved measurements in transparent and absorbing CS_2 demonstrate that self-focusing of light beams at high intensities is strongly influenced by stimulated Raman and Brillouin scattering. Both processes reduce the laser power in the liquid cell and limit the time-duration of the self-focusing action.

VI. Summary

Numerical solutions of the wave equation were obtained for different initial conditions (divergence, diameter, and power of the light beam). The results were compared with experimental investigations of self-focusing in transparent and absorbing CS_2 and molten para-di-chlorobenzene. Both the spatial and temporal development of the self-focusing process was determined.

With increasing laser power self-focusing leads to a strong increase of the intensity in the center of the beam while its outer portions are less affected. Measured and calculated intensity distributions over the beam cross section are in quantitative agreement. Due to the self-focusing action the beam diameter at the end of the medium decreases with increasing laser power to the limiting value of 5 μ. The experimental results in CS_2 and para-di-chlorobenzene are in good agreement with numerical calculations both for a parallel and a divergent incident laser beam. The drastic influence of beam divergence and nonlinearity of refractive index was demonstrated clearly by our measurements. In strongly absorbing liquids (power transmission of the medium only a few percent) the strong reduction of beam diameter due to self-focusing action was found to agree well with theory.

The time-resolved investigations of the self-focusing process in CS_2 showed good agreement between

theory and experiments; they allowed the following conclusions. If a laser giant pulse is sent through the liquid the beam diameter is reduced during its path through the cell due to self-focusing. The diameter at the exit window, which decreases with increasing laser power, follows quasistationarily the instantaneous laser power. For low incident laser power, the diameter increases again after the power has passed its peak value. At high laser power, stimulated Raman scattering in the forward and backward direction and stimulated Brillouin scattering occur, since the self-focused beam diameter is strongly reduced leading to a drastic increase of intensity. These scattering processes in the backward direction attenuate rapidly the laser power and limit the time duration of the self-focusing action.

The authors wish to thank Professor W. KAISER for his continuous interest in this work and for many valuable discussions and Dr. G. K. BORN for a reading of the manuscript.

A New Type of Apparatus for the Determination of the Thermal Diffusion Factor

W. A. OOST * and A. HARING

FOM-Instituut voor Atoom- en Molecuulfysica, Kruislaan 407, Amsterdam/Wgm.

(Z. Naturforsch. **25 a**, 1879—1882 [1970]; received 11 September 1970)

In this article an apparatus is presented which gives a precisely known multiplication of the elementary effect in thermal diffusion experiments, avoiding the drawbacks of the swing-separator (Trennschaukel). This is achieved by using a different method of concentration nivellation than customary with the swing-separator, viz. thermosyphon action.

Introduction

Of the three types of apparatus, in regular use in thermal diffusion experiments, only two, the two-bulb apparatus and the swing-separator, designed by CLUSIUS and HUBER [1] are fitted for a precise determination of the thermal diffusion factor, whereas the thermal diffusion column, invented by CLUSIUS and DICKEL [2] is more or less a production apparatus, very useful for the attainment of high separations between the components of a gaseous mixture, but too complicated in its functioning to permit a precise determination of the thermal diffusion factor from these separations. The need for a second apparatus beside the basic and well understood two-bulb apparatus arises from the fact that thermal diffusion is a second order effect and as such can be very small, making the separation obtained in a two-bulb apparatus too small for the evaluation of the thermal diffusion factor with a reasonable accuracy.

The swing-separator, on the other hand, has its own drawbacks. It produces a separation which is meant to be an exactly determined power of the elementary separation as measured in a two-bulb apparatus. This is done by coupling a number of two-bulb apparatuses (tubes) by means of pieces of capillary tubing, which connect the cold side of tube number n to the hot side of tube $n+1$ and pumping the gas to and fro through these capillaries, so that a concentration nivellation takes place at both ends of each capillary. In this way an exactly known multiplication of the elementary separation takes place. However, as VAN DER WAERDEN [3] has shown, several disturbing factors make this type of apparatus less ideal than it looks at first sight. Under optimal conditions the finite pumping speed leaves a concentration difference at both ends of each capillary, due to back diffusion in the capillary. Raising the pumping speed would diminish this error, but introduces an other one: the gas masses flowing in and out each separation tube disturb the thermal and concentration equilibrium in these tubes. This can be seen in the following way: hot gas from the upper side of one tube is introduced into the cold side of the next one and vice versa and the entering gas causes turbulence in the (supposedly) stationary state of the mixture.

Reprints request to Prof. J. KISTEMAKER, FOM-Instituut voor Atoom- en Molecuulfysica, Kruislaan 407, *Amsterdam-Watergraafsmeer*, Niederlande.

* Now at the Royal Netherlands Meteorological Institute (KNMI), De Bilt, Netherlands.

[1] K. CLUSIUS and M. HUBER, Z. Naturforsch. **10 a**, 230 [1955].
[2] K. CLUSIUS and G. DICKEL, Z. Phys. Chem. **B 44**, 397 [1939].
[3] B. L. VAN DER WAERDEN, Z. Naturforsch. **12 a**, 583 [1957].